World Academy of Science, Engineering and Technology
International Journal of Computer and Information Engineering
Vol:15, No:11, 2021

Automatic Classification of the Stand-to-Sit Phase in the TUG Test Using Machine Learning

Y. A. Adla, R. Soubra, M. Kasab, M. O. Diab, A. Chkeir

***Abstract*—**Over the past several years, researchers have shown a great interest in assessing the mobility of elderly people to measure their functional status. Usually, such an assessment is done by conducting tests that require the subject to walk a certain distance, turn around, and finally sit back down. Consequently, this study aims to provide an at home monitoring system to assess the patient's status continuously. Thus, we proposed a technique to automatically detect when a subject sits down while walking at home. In this study, we utilized a Doppler radar system to capture the motion of the subjects. More than 20 features were extracted from the radar signals out of which 11 were chosen based on their Intraclass Correlation Coefficient (ICC > 0.75). Accordingly, the sequential floating forward selection wrapper was applied to further narrow down the final feature vector. Finally, five features were introduced to the Linear Discriminant Analysis classifier and an accuracy of 93.75% was achieved as well as a precision and recall of 95% and 90% respectively.

***Keywords*—**Doppler radar system, stand-to-sit phase, TUG test, machine learning, classification.

I. Introduction

OVER the past few decades, researchers have shown a great interest in human gait analysis and its various applications. When it comes to gerontology, physicians are interested in studying the motion of elderly subjects to detect any signs of mobility impairment or decline [1]. Therefore, several clinical tests were designed and implemented to assess subjects' mobility and frailty based on the gait analysis.

During clinical evaluations, subjects are prompted to complete a series of tasks based on the requirements of each test. To illustrate, the Timed Up and Go (TUG) test is one of the most common clinical assessments where subjects are asked to stand up from the chairs they were sitting on, walk forward for a distance of 3 meters, turn around, and sit back down in their seats [2]. During the TUG test, two transfer phases are performed: Sit-to-Stand phase and the Stand-to-Sit phase. The Stand-to-Sit phase can be further divided into two sub-phases: the turning to sit phase and the sitting down phase. An example on how a radar signal during the TUG test can be segmented is seen in Fig. 1, where:

- T1 corresponds to the Standing phase
- T2 corresponds to the Turning to Sit phase
- T3 corresponds to the Stabilization phase (the phase where the subject stabilizes him/herself after turning around and just before sitting down). It is worthy to note that this phase may be crucial in determining and studying the stability and frailty of elderly people.
- T4 corresponds to the Sitting down phase

Meanwhile, the Dynamic Gait Index (DGI) test assesses subjects' functional stability while performing eight tasks that range from walking and turning to crossing over and around obstacles [1].

Most of these clinical tests take place in specialized clinics under the supervision of trained physicians. Nevertheless, in order to improve the evaluation of the functional status of seniors, continuous monitoring of their gait is needed. In fact, when clinicians are provided with constant updates and information on their patients, they can tell if subjects are at higher risk of adverse outcomes such as falling, physical disability, cognitive impairment, etc.

Based on all of the above, various technological systems were built and implemented to provide elderly with constant walking supervision in the comfort of their own homes. Such systems mostly require installing cameras inside the subject's home or wearing different sensors [3]. Although these systems have their own advantages, many problems arise from their use. To exemplify, camera-based systems may invade and violate a person's privacy. Additionally, an elder might forget to wear the necessary sensors that the monitoring system depends on to extract useful parameters and information [1]. Thus, many researchers are nowadays working on designing new techniques that are much more accurate while keeping in mind the practicality of the system and the patients' privacy.

Therefore, this paper proposes a novel technique for an at home monitoring system that automatically detects the two sub-phases (turning to sit phase and the sitting down phase) in the Stand-to-Sit phase during the motion of the subject. A Doppler radar was utilized in this study as it is not affected by surrounding light, does not require the user to wear any special equipment, is effective while remaining cost friendly, and finally provides the user with the needed privacy [1].

The remainder of this paper is organized as follows: Section II tackles the experimental protocol and the followed methodology. Then, Section III discusses the results followed by the conclusion and future perspectives in section IV.

Aly Chkeir is with the University of Technology of Troyes (corresponding author, e-mail: aly.chkeir@utt.fr).

Yasmine Abu Adla, Racha Soubra, Milana Kasab, Aly Chkeir are with LIST3N/M2S, University of Technology of Troyes, France (e-mails: (yasmine.abu_adla@utt.fr, racha.soubra@utt.fr, milana.kasab@utt.fr).

Mohamad O. Diab is with the Rafik Hariri University, Lebanon (e-mail: diabmo@rhu.edu.lb).

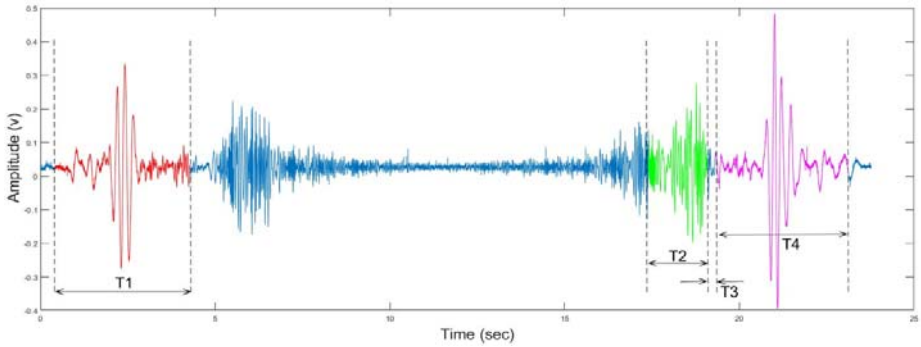

Fig. 1 Segmented Radar Signal during the TUG Test

II. Methodology

A. Experimental Protocol

Ten healthy participants, five females and five males, age ranging between 22 and 27 years, volunteered to participate in the conducted study. They were given a detailed description on the experimental protocol as well as the motivation of the study at hand. Since the aim of this study is to detect the Stand-to-Sit phase in elderly people, the participants were asked to watch a one-minute video of an older adult performing the TUG test and mimic them several times as practice trials. After making sure that the subjects were familiar with the TUG test and what they are expected to do, each subject was asked to perform the TUG test in a slow manner four consecutive times. The entire experiments were performed in the UTT well-equipped laboratory as shown in Fig. 2.

In order to obtain the ground truth reference data for every trial, a 3D motion tracking system, known as the Vicon system, was utilized. The Vicon system is an optoelectronic system that depends on infrared cameras and reflective markers placed in the subject's body. The Vicon cameras emit infrared light and receive the reflected waves from the markers. Based on the set origin and the reflected wave, the position of the subject can be computed in the x, y, and z directions. In this study, eight Vicon cameras were used along with four reflective markers placed on the left and right shoulder as well as the left and right toe. The system was calibrated before the beginning of the experiment.

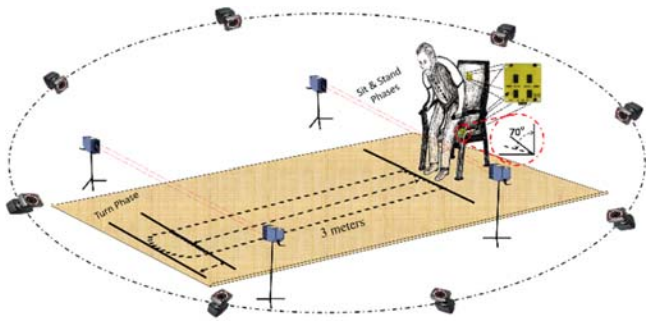

Fig. 2 Experimental Setup

In this study, an X-band Doppler Motion Detector of frequency 10.587 GHz was utilized [4]. After performing a set of experimental trials, it was decided that the radar would be placed on the edge of the seat, tilted outward at a 20-degree angle, and positioned at a 70-degree angle with respect to the x-axis. This system is used to locate and calculate different gait parameters based on the principle of transmitted and reflected electromagnetic waves. To illustrate, the radar emits an electromagnetic wave and receives a reflected signal after it bounces off a moving target. Based on the Doppler effect, the speed of the target can be calculated as seen in (1)

$$v = \frac{\Delta f \times c}{2 f_e} \quad (1)$$

where v is the target speed, c is the speed of light in vacuum ($3 \times 10^8\ m/s$), Δf is the difference between the transmitted and the received frequency, and f_e is the frequency of the signal emitted by the radar [5].

The radar output was connected to an electronic circuit to filter out noise and amplify its amplitude. Initially, based on the location of the radar and how close it would be near the subject while sitting, a gain of 45 was used. As for the filters, the radar output was introduced to a band pass filter with cut-off frequencies of 2 Hz and 1200 Hz. In fact, the cut-off frequencies were set approximately based on the minimum ($v_{min} = 0.075\ m/s$) and maximum walking speed ($v_{max} = 1.5\ m/s$) of an individual [1]. However, in order to compensate for the speed of the limbs, which can reach up to 500 Hz, and to leave a certain margin of error, the cut-off frequencies were set to 2 Hz and 1200 Hz.

B. Pre-Processing

In this study, the processing of the radar signal was done using two different techniques.

Firstly, it was proposed to convert the radar signals into a Waveform Audio File to extract spectral features found strictly in audio signals. In fact, based on the Doppler effect, the Doppler Frequency shift Δf seen in the backscattered radar signal of a moving person is equal to $2v/\lambda$, where v is the velocity of the subject and λ is the wavelength of the emitted radar signal. The Doppler frequency shift (Δf_D) due to the motion of the human torso is between 190 and 30 Hz, which lies in the frequency band of audio signals. Although swinging human limbs cause a larger shift in the Doppler Frequency, the frequencies are still within the audio frequency band. Thus, Doppler signal received after backscattering from the motion of a subject can be related to audio signals [6]. Furthermore, as

seen in Fig. 3, the radar and audio signal share common characteristics and parameters which allows us to apply speech processing on radar signals. In our study, the recorded radar signals were converted to a ".wav" file in order to extract the necessary features.

In order to visualize the acquired signals in the time-frequency domain, the Continuous Wavelet Transform (CWT) was applied to the Doppler signals using the "bump" wavelet [1]. Since this study aims to detect the transfer phase of a moving subject, the maximum energy point was extracted from the CWT matrix at each instant. Hereafter, the Doppler Equation was applied to the obtained signal to calculate the speed of the subject.

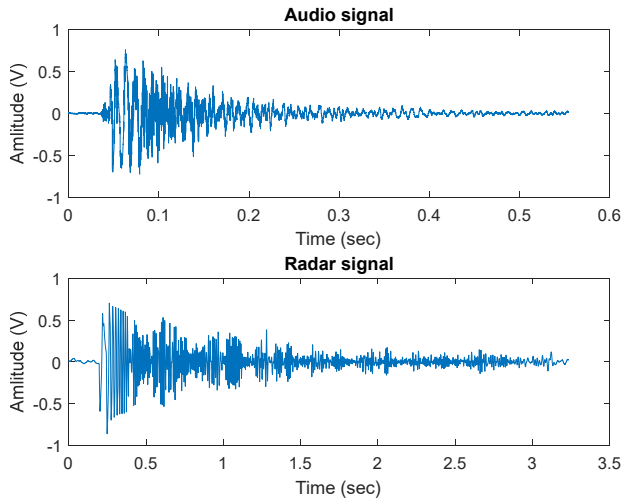

Fig. 3 Comparison between Audio Signal (on top) and Radar Signal (bottom)

C. Feature Extraction

More than 20 time domain, frequency domain and time-frequency domain features were extracted from our radar signals as follows:

1. Time Domain Features: Mean [7], Variance [7], Kurtosis [8], Skewness [8], Sequence Period [9], Root Mean Square (RMS) [10], Autocorrelation [11], and Partial Autocorrelation [11], and Zero Crossing Rate [12].
2. Frequency Domain Features: Median and Mean frequency [13], Spectral Bandwidth [14], [20], Spectral Roll-off [15], [20], Spectral Flatness [18], p20], Spectral Entropy [18], and Spectral Contrast [19].
3. Time-Frequency Domain Features: Speed and Acceleration were computed after applying the CWT to the radar signal, extracting the maximum energy points, and then applying Doppler Equation. Chroma Short Time Fourier Transform (STFT) [16], Chroma Constant-Q transform (CQT) [16], Spectral Centroid [14], Mel Spectrogram [17], and Mel Frequency Cepstral Coefficient (MFCC) [18].

D. Feature Selection

Feature selection is selecting a subset of features that include only the relevant and essential features. In this stage, the low-reliable features are removed so that the performance of the classifier is enhanced and computation time is reduced [21].

Firstly, it was of utmost importance to select the reliable and consistent features; hence, we propose a feature selection technique based on the ICC outcomes. In fact, the ICC measures how repeatable and reliable a feature is [22], [23]. In this research, the ICC was computed using the 2-way random effect model, a k-measurement type, and an absolute agreement estimation. The preceding model was chosen since the sample of raters is randomized and it is essential for the outputs to have an agreement between them [24]. Regarding the selected type, the intended measurement protocol is planned to be done in actual applications through a series of measurements. Thus, the ICC can be calculated as in (2).

$$ICC = \frac{MS_R - MS_E}{MS_R + \frac{MS_C - MS_E}{n}} \quad (2)$$

where, MS_R is the mean square of the rows, MS_E is the mean square error, MS_C is the mean square of the columns, and n is the number of subjects.

After the initial screening of the features using the ICC, a wrapper was applied to further narrow down the final feature vector. To illustrate, wrapper methods select the subset of features based on the learning algorithm's performance [25]. In this work, we applied the Sequential floating forward selection (SFFS) wrapper to the chosen features using nine different classifiers. The SFFS goes through three basic phases [25]:

1. **Inclusion:** the SFFS starts with an empty set of features (X = 0) then, it takes a step forward by inserting the most significant feature concerning X.
2. **Conditional exclusion:** the SFFS finds the least significant feature k in X. If that feature has been just added, then it is kept and the algorithm goes back to step 1. Else, feature k is excluded and the algorithm proceeds to step 3.
3. **Continuation of conditional exclusion:** the least significant feature is found again in X. If its removal will leave at least two features in X and will cause a larger value for the feature selection criterion function J(X), then the SFFS removes that feature and repeats the same steps. Whenever these two conditions cease to exist, the SFFS returns to step 1 until a predetermined number of features is reached.

In our research, the SFFS was applied to nine classifiers that are commonly used when classifying radar and electromagnetic signals [26]. The list of used classifiers can be seen below. An example of how the SFFS works when applied to one of these classifiers can be seen in Fig. 4.

1. Decision Tree (DT)
2. Random Forest (RF)
3. Linear Discriminant Analysis (LDA)
4. Quadratic Discriminant Analysis (QDA)
5. Logistic Regression (LR)
6. Support Vector Machine with a linear kernel (SVM)

7. K-nearest neighbors (KNN)
8. Naïve Bayes (NB)
9. Multi-layer Perceptron (MLP)

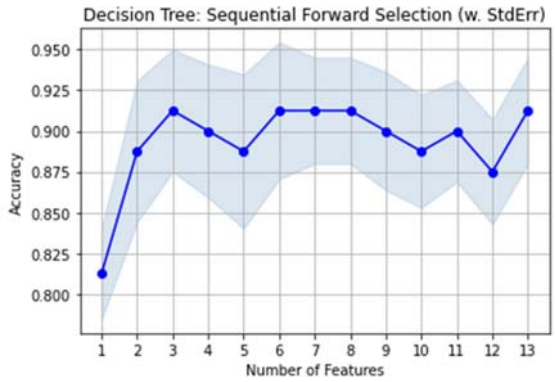

Fig. 4 SFFS applied on the Decision Tree Classifier

E. Training and Testing the Models

After applying the SFFS, the feature vector that yielded the highest accuracy was considered for each classifier. Hereafter, the model was trained and tested on its corresponding subset of features using 10-fold cross-validation.

III. Results and Discussion

The TUG test performed by the participants can be sectioned into three transfer phases, as mentioned earlier; thus, as seen in Table I, the ICC was computed for all the features in the three phases of a TUG test: Standing, Turning to sit, and Sitting down. The bold values found in the table refer to reliable features since ICC values between 0.5 and 0.75, 0.75 and 0.9, and 0.9 and 1, respectively, indicate moderate, good, and excellent reliability [24].

TABLE I
ICC Values of Reliable Features during Different Phases

Features	Standing	Turning to Sit	Sitting Down
Zero Crossing Rate	0.85	0.40	0.89
Root Mean Squared	0.90	0.87	0.80
MFCC	0.90	0.73	0.82
Spectral Contrast	0.78	0.85	0.87
Spectral Flatness	0.34	0.85	0.84
Mel Spectrogram	0.88	0.83	0.68
Spectral Roll-off	0.82	0.69	0.90
Spectral Bandwidth	0.78	0.86	0.89
Spectral Centroid	0.78	0.76	0.91
Kurtosis	0.75	0.63	0.62
Mean	0.83	0.84	0.62
Variance	0.78	0.88	0.65
Median Frequency	0.78	0.78	0.95
Peak2RMS	0.79	0.73	0.83
RMS	0.85	0.48	0.72
Skewness	0.84	0.72	0.96
Sequence Period	0.89	0.82	0.96
Spectral Entropy	0.82	0.79	0.86
Partial Correlation	0.80	0.76	0.88
Auto Correlation	0.80	0.78	0.87

Since the main aim of this work is to detect the different phases, but namely, the turning to sit and the sitting phase, two different feature vectors were taken into consideration. To exemplify, the first feature vector consisted of features that were reliable in all three phases, while the second vector included parameters that were reliable in the turning to sit and sitting down phase. The two feature vectors were introduced to the SFFS wrapper based on all nine classifiers mentioned above. The results of the SFFS are shown in Tables II and III where the highest accuracies achieved by the classifier are mentioned as well as their corresponding number of features for the first and second feature vector, respectively. In fact, Table II shows how well the classifier performed when classifying the three phases while Table III depicts how well the models performed when separating only two instances.

TABLE II
SFFS Results Based on Different Classifiers (All Phases)

Classifier	Accuracy (%)	Size of Feature Vector
Decision Tree	75	5
Random Forest	79.16	6
Quad. Discriminant Analysis	70.83	2

TABLE III
SFFS Results Based on Different Classifiers (Turn and Sit Phase)

Classifier	Accuracy (%)	Size of Feature Vector
Decision Tree	91.25	3
Random Forest	93.75	11
Linear Discriminant Analysis	93.75	5
Quad. Discriminant Analysis	90	5

After finding the classifiers that performed the best in terms of accuracy, each feature vector was taken and reintroduced into the studied model to train and test using 10-fold cross-validation. The results of this step are shown in Tables IV and V.

TABLE IV
Evaluation of Classifiers (All Phases)

Classifier	Accuracy (%)	Precision	Recall
Decision Tree	56	57	57
Random Forest	76.5	76	79
Quad. Discriminant Analysis	70	69.96	69

TABLE V
Evaluation of Classifiers (Turning and Sitting Down Phase)

Classifier	Accuracy (%)	Precision (%)	Recall (%)
Decision Tree	92.5	91.7	97.5
Random Forest	89	92.6	95
Linear Discriminant Analysis	93.75	95.5	90
Quad. Discriminant Analysis	92.5	90.6	90

As seen in the preceding tables, the classification models were able to perform well when classifying the turning to sit and sitting down phase in the TUG test. That is due to the fact

that the standing phase, which is very similar to the sitting down phase, is not taken into consideration. Therefore, since in previous works, the standing phase was detected using different techniques, we can neglect it and focus on the remaining two phases. Thus, it was evident that the LDA classifier had the best performance when it came to distinguishing the turning to sit and sitting down phase.

IV. Conclusion and Future Perspectives

To wrap things up, this work investigates the possibility of building a Machine Learning model that distinguishes the two sub-phases when a person sits down. This was done by extracting various features from the radar signal and filtering them out based on their reliability and their contribution to the learning process. Then, several classifiers were tested and the one with the best performance was selected.

As for detecting the exact instants at which the subject begins to turn around to sit and when he/she starts to sit down, we aim to use regression to find a generalized equation for motion of a subject during the entire TUG test. Through modeling, we will be able to find an equation upon which we can detect the desired instances.

Acknowledgment

This work was supported by the GRAND-EST Region, the European Regional Development Fund (FEDER) and DOMITYS Group.

References

[1] R. Soubra, A. Chkeir, F. Mourad-Chehade, D. Alshamaa, B. Dauriac and J. Duchene, "Doppler Radar System for an Automatic Transfer Phase Detection Using Wavelet Transform Analysis," in *3rd International Conference on Bio-engineering for Smart Technologies (BioSMART)*, Paris, France, 2019.

[2] Podsiadlo, D. and S. Richardson, The timed “Up & Go”: a test of basic functional mobility for frail elderly persons. Journal of the American geriatrics Society, 1991. 39(2): p. 142-148.

[3] Sprint, G., D.J. Cook, and D.L. Weeks, Toward automating clinical assessments: a survey of the timed up and go. IEEE reviews in biomedical engineering, 2015. 8: p. 64-77.

[4] Microwave Solutions Ltd. Available from: https://www.microwave-solutions.com/datasheets.

[5] C. Neipp, A. Hernández, J. Rodes, A. Márquez, T. Beléndez and A. Beléndez, "An analysis of the classical Doppler effect," *European Journal of Physics,* vol. 24, 2003.

[6] P. Molchanov, J. Astola, K. Egiazarian, Totsky and Alexander, "Classification of ground moving targets using bicepstrum-based features extracted from Micro-Doppler radar signatures," *EURASIP Journal on Advances in Signal Processing,* 2013.

[7] S. Hozo, B. Djulbegovic and H. I, "Estimating the mean and variance from the median, range, and the size of a sample," *BMC Medical Research Methodology*, 2005.

[8] S. Yusoff and Y. Wah, "Comparison of conventional measures of skewness and kurtosis for small sample size," in *Statistics in Science, Business, and Engineering (ICSSBE)*, 2012.

[9] Q. Yuan, J. Shang, X. Cao, C. Zhang, X. Geng and J. Han, "Detecting Multiple Periods and Periodic Patterns in Event Time Sequences," in *2017 ACM on Conference on Information and Knowledge Management*, 2017.

[10] P. Petrovic, "Root-mean-square measurement of periodic, band-limited signals," in *Instrumentation and Measurement Technology Conference (I2MTC), IEEE International*, 2012.

[11] Z. Ke and Z. Zhang, "Testing autocorrelation and partial autocorrelation: Asymptotic methods versus resampling techniques," *British Journal of Mathematical and Statistical Psychology,* vol. 7, no. 1, pp. 96-116, 2017.

[12] M. Akçay and K. Oguz, "Speech emotion recognition: Emotional models, databases, features, preprocessing methods, supporting modalities, and classifiers," *Speech Comminucation,* vol. 116, pp. 56-76, 2020.

[13] T. Freeborn, "Fatigue monitoring techniques using wearable systems," in *Wearable Sensors (Second Edition) Fundamentals, Implementation and Applications*, Academic Press, 2021, pp. 575-592.

[14] T. Giannakopoulos and A. Pikrakis, "Audio Features," in *Introduction to Audio Analysis - A MATLAB Approach*, Academic Press, 2014, pp. 59-103.

[15] G. Peeters, "A large set of audio features for sound description (similarity and classification) in the CUIDADO project," 2004.

[16] A. Shah, M. Kattel, A. Nepal and Shrestha, "Chroma Feature Extraction," in *Chroma Feature Extraction using Fourier Transform*, 2019.

[17] B. Zhang, J. Leitner & S. Thornton, "Audio Recognition using Mel Spectrograms and Convolution Neural Networks," 2019.

[18] L. Muda, M. Begam and I. Elamvazuthi, "Voice Recognition Algorithms using Mel Frequency Cepstral Coefficient (MFCC) and Dynamic Time Warping (DTW) Techniques," *JOURNAL OF COMPUTING,* vol. 2, no. 3, 2010.

[19] D. Mitrović, M. Zeppelzaue and C. Breiteneder, "Features for Content-Based Audio Retrieval," in *Advances in Computers*, ELSEVIER, 2010, pp. 71-150.

[20] J. Yang, F.-L. Luo and A. Nehorai, "Spectral contrast enhancement: Algorithms and comparisons," *Speech Communication,* pp. 33-46, 2002.

[21] E. Karabulut, S. Ozel and T. İbrikçi, "A comparative study on the effect of feature selection on classification accuracy," in *First World Conference on Innovation and Computer Sciences (INSODE 2011)*, 2012.

[22] McGraw, K.O. and S.P. Wong, Forming inferences about some intraclass correlation coefficients. Psychological methods, 1996. 1(1): p. 30.

[23] Shrout, P.E. & J.L. Fleiss, Intraclass correlations: uses in assessing rater reliability. Psycho. bulletin, 1979. 86(2): p. 420.

[24] T. Koo and M. Li, "A Guideline of Selecting and Reporting Intraclass Correlation Coefficients for Reliability Research," *Journal of Chiropractic Medicine,* 2016.

[25] N. El Aboudi and L. Benhlima, "Review on wrapper feature selection approaches," in *International Conference on Engineering & MIS (ICEMIS)*, 2016.

[26] P. Lang, X. Fu, M. Martorella, J. Dong, R. Qin, X. Meng and M. Xie, "A Comprehensive Survey of Machine Learning Applied to Radar Signal Processing," 2020.